ICARUS **132,** 185–195 (1998)
ARTICLE NO. IS985904

Regolith and Megaregolith Formation of H-Chondrites: Thermal Constraints on the Parent Body

Glen Akridge, Paul H. Benoit, and Derek W. G. Sears

Cosmochemistry Group, Department of Chemistry and Biochemistry, University of Arkansas, Fayetteville, Arkansas 72701
E-mail: cosmo@cavern.uark.edu

Received July 31, 1997; revised December 15, 1997

Spectral reflectivity data and its location near an orbital resonance suggest that Asteroid 6 Hebe may be the source body for H-chondrites, the second largest meteorite group. Recent spacecraft images of asteroids and theoretical modeling indicate that, contrary to previous ideas, asteroids can retain thick regoliths. We model the thermal evolution of a Hebe-sized object coated with a thick insulating regolith and heated by ^{26}Al and other long-lived radionuclides. The heat conduction equations for spherically symmetric objects were solved using finite-difference approximations. We assumed a three-layer structure with regolith and megaregolith overlying a rocky core. The three layers differed in bulk density, porosity, and thermal conductivity. Interior peak temperatures were set to match metamorphic temperatures of H6 chondrites.

The regolith has a major influence on thermal history, and the results are very different from those for a simple rocky body published by various authors. Regolith insulation produces a uniform interior peak temperature of ~1250 K and moves the petrographic type boundaries close to the surface of the parent body. Petrologic types 3–6 can be produced within 10 km of the asteroid's surface with only moderate (~1 km) regolith thicknesses. The calculations indicate that H4–H6 formation would be consistent with the cooling rate estimates and Pb–Pb formation ages if the material originated in the near surface regions. We suggest that many if not all H-chondrites could have been formed in a megaregolith and thick regolith. Their observed properties are consistent with this environment, especially the abundance of regolith breccias and H-chondrites of all petrologic types with implanted solar wind gases.

Key Words: **asteroids; meteorites; regoliths; thermal histories; surfaces, asteroidal.**

INTRODUCTION

Recent work on the orbital dynamics of material ejected from Asteroid 6 Hebe and the spectral characteristics of the asteroid suggest that it might be a reasonable source for the H-chondrites. Farinella *et al.* (1993) and Morbidelli *et al.* (1994) have suggested that Hebe's location near the ν_6 and 3:1 resonances make it an ideal candidate for producing Earth-crossing meteoroids. The chaotic zones associated with these resonances can act as escape hatches that send impact ejected fragments toward the inner solar system. H-chondrites represent the second largest class of meteorites falling to Earth (Sears and Dodd 1988). The undifferentiated surface of Hebe appears spectrally similar to ordinary chondrites (Migliorini *et al.* 1997) and Gaffey (1996) concluded that Hebe's surface mineralogy is sufficiently similar to H-chondrites to make it the potential source body for H-chondrites and IIE irons. The spectra of Hebe appear to be enriched in FeNi metal when compared to H-chondrites, a feature attributed to impact melt "pools" of metal on the planet's surface (Gaffey and Gilbert 1997). Keil *et al.* (1997), however, suggest that melt volumes on Hebe-sized objects are too low to account for melt pools. The lunar regolith, the closest comparable body for which we have data, contains impact melt products that compose up to 65 vol% of the surface (McKay *et al.* 1991).

Nearly all meteorites display evidence of having experienced significant heating, most probably as part of the thermal history of the parent body. The existence of achondritic and iron meteorites indicates that heating was enough to melt and differentiate at least parts of some parent bodies. Chondritic meteorites, however, escaped the melting process but experienced a large range of peak temperatures. Ordinary chondrites range from nearly unmetamorphosed type 3 to highly metamorphosed and mineralogically equilibrated type 6. Petrographic types 3, 4, 5, and 6 most probably experienced peak temperatures of 870, 970, 1020, and 1220 K, respectively (McSween *et al.* 1988).

In an attempt to explain the range of metamorphism observed in ordinary chondrites and make deductions about parent body sizes, numerical models have used the estimated peak temperatures, cooling rates, and formation time intervals as constraints. These models can essentially be categorized by their heating mechanisms. Heat production from electromagnetic induction during an intense

0019-1035/98 $25.00

early solar wind has been suggested (Herbert *et al.* 1991), but may require unrealistic solar wind fluxes through the ecliptic plane and higher electrical conductivities than those observed in chondritic rocks (Wood and Pellas 1991). Long-lived radionuclides U, Th, and K do not provide an effective heat source because the rate of heat loss by asteroid-sized bodies nearly equals the rate of heat generation by radionuclides, so that maximum temperatures achieved are <800 K (Yomogida and Matsui 1984). Short-lived ^{26}Al is a more reasonable heat source, and excess daughter product ^{26}Mg found in calcium–aluminum inclusions (CAI) in the CV3 Allende (Lee *et al.* 1976) and aluminum-rich chondrules and CAI in ordinary chondrites (Russell *et al.* 1996), indicate that it might be a viable heat source in some cases. Models based upon ^{26}Al decay have provided estimates of parent body size, cooling rates, and formation times (e.g., Herndon and Herndon 1977; Minster and Allègre 1979; Miyamoto *et al.* 1981; Bennett and McSween 1996; Akridge *et al.* 1997). The decay of ^{60}Fe is another possible heat source in the early solar system (Shukolyukov and Lugmair 1992), but rates of heat production are a factor of ~10 lower than for ^{26}Al (Grimm and McSween 1993). Collisional heating has also been proposed (e.g., Rubin 1995), and Sears *et al.* (1997) concluded that impact heating was responsible for eucrite metamorphism.

The potential for thick regolith development on asteroids has been confirmed by Galileo spacecraft images of Gaspra and Ida (Carr *et al.* 1994; Belton *et al.* 1994). Both asteroids contain regoliths tens to hundreds of meters thick despite their small size (radius < 20 km). These observations have resulted in considerable revision to theoretical models that predicted little or no regolith buildup on small bodies. Early regolith production models concluded that regolith on small bodies was limited to <100 m thickness (Langevin and Maurette 1980) or entirely absent (Housen *et al.* 1979), but more recent calculations have shown that even small bodies can retain significant amounts of ejecta if they have low strength (Housen 1992; Asphaug and Nolan 1992). Regolith buildup on asteroids is dependent on the fraction of ejecta retained by the body. Thus, a Hebe-sized object (radius = 93 km) would be expected to have a thicker regolith because of its larger gravity field than Gaspra or Ida, assuming a similar mechanical strength in the surface regions.

This paper presents numerical calculations performed for a Hebe-sized asteroid with H-chondrite properties using ^{26}Al as the heat source. Unlike previous work on chondrite parent body thermal history, we have considered the effects of regolith insulation. We show that a thick regolith can substantially reduce parent body cooling rates so that meteorites of all petrographic types might have been produced in the megaregolith or regolith.

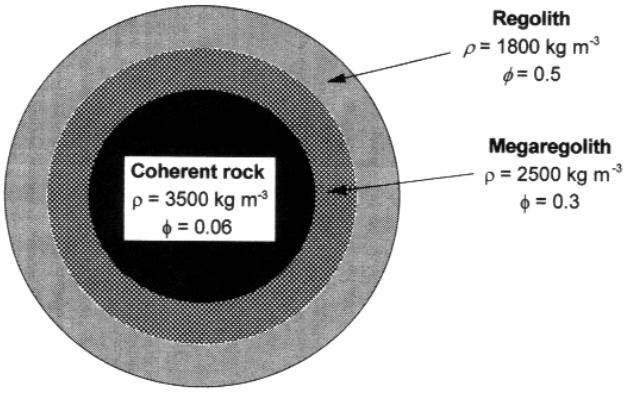

FIG. 1. Three layer modeled structure of Hebe with typical values for density (ρ) and porosity (ϕ) used in the calculations. Total radius of modeled Hebe = 100 km.

THERMAL MODEL

We assume a homogenous distribution of ^{26}Al, ^{60}Fe, ^{40}K, ^{232}Th, ^{235}U, and ^{238}U throughout the parent body. Initial internal temperatures are assumed using blackbody characteristics for an object in the present asteroid belt. The surface temperature is assumed to be constant over the course of the numerical calculations. Appropriate values (discussed below) for density and porosity were chosen for the mantle, megaregolith, and regolith (Fig. 1). Calculations begin at the center of Hebe and proceed outward using the appropriate material properties for each structural zone. If volume changes are neglected, then the heat conduction equation for a spherically symmetric body can be used to determine temperature for any position and time (Allan 1955),

$$\frac{\partial T}{\partial t} = \frac{1}{r^2 \rho C_p} \frac{\partial}{\partial r}\left[r^2 K \frac{\partial T}{\partial r}\right] + \frac{A(t)}{\rho C_p}, \tag{1}$$

where T is the temperature, ρ the material density, C_p the heat capacity, K the thermal conductivity, $A(t)$ the rate of heat generation, and t and r are the time and radial position within the body, respectively.

The equation becomes a nonlinear partial differential equation whenever thermal conductivity varies with temperature. MacDonald (1959) solved Eq. (1) numerically for the nonlinear case using finite difference approximations for the first and second derivatives. The approximating equation for the center of the body is

$$T_0^{n+1} = T_0^n + \frac{\Delta t}{\rho_0 C_p (\Delta r)^2}\left[6K_0(T_1^n - T_0^n) + (K_1 - K_0)(T_1 - T_0)\right] + \frac{A_0 \Delta t}{\rho_0 C_p} \tag{2}$$

and throughout the body is

$$T_m^{n+1} = T_m^n + \frac{\Delta t}{\rho_m C_p}\left\{\frac{1}{m(\Delta r)^2}\left(\left[\frac{m}{4}(K_{m+1} - K_{m-1}) + (m+1)K_m\right]T_{m+1}^n - 2mK_mT_m^n - \left[\frac{m}{4}(K_{m+1} - K_{m-1}) - (m-1)K_m\right]T_{m-1}^n\right) + A_m\right\}, \quad (3)$$

where m and n are positional and time steps, respectively. For the boundaries between the regolith, megaregolith, and the interior the proper equation is

$$T_m^{n+1} = T_m^n + \frac{\Delta t}{\rho_m C_p}\left\{\frac{1}{m(\Delta r)^2}\left(\left[\frac{m}{4}(K_{m+1} - K_{m-1}) + mK_{m+1} + K_m\right]T_{m+1}^n - m(K_{m+1} + K_m)T_m - \left[\frac{m}{4}(K_{m+1} - K_{m-1}) - (m-1)K_m\right]T_{m-1}^n\right) + A_m\right\}. \quad (4)$$

We calculated a new temperature for each positional step within the body. Positional increments were generally set between 250 and 500 m. To avoid instabilities in the calculations, the time interval given by

$$\Delta t = \frac{\rho C_p (\Delta r)^2}{2K} \quad (5)$$

was set as a function of the positional step size Δr and K of the interior region (Reynolds *et al.* 1966). The numerical calculations assume the regolith and megaregolith thicknesses to be constant, typically between 0.5 and 3 km in depth. Cratering on Hebe would create localized areas of thick and thin regolith thicknesses and differential heat flow near the surface. Our model reflects a global average of regolith/megaregolith thickness. The original radius of Hebe is assumed to have been 100 km, about 7% greater than its present value, assuming some mass loss due to impact.

Sintering in the outer layers of the body has not been considered since the sintering process is not well understood in regard to meteorite parent bodies. Wood (1979) proposed that sintering of a dusty 20 km chondritic asteroid would increase the thermal conductivity of the material and result in volume shrinkage. This model reflects sintering characteristics on Earth where fusion between grains can occur at temperatures >800 K. For asteroid surfaces, impact communition may partially off set any sintering and it is clear from the textures of the dark matrix of regolith breccia chondrites that surface processes can create and maintain unconsolidated materials. Heating of the regolith from ^{26}Al decay would occur for only a few Ma after accretion, a time when impact bombardment of the surface is expected to be high. The abundance of regolith breccias containing H4–H6 material (Bunch and Rajan 1988) is an indication that the lithification process for these meteorites was postmetamorphism. It is also unclear how sintering affects highly porous material on a low-gravity body. For asteroid-sized bodies in which the gravity field is 100–1000 times lower than for Earth, sintered material may not be compacted into a more thermally conductive rock. Until sintering experiments can be conducted under these conditions, we feel that there is no strong argument for significant sintering effects on asteroid surface material immediately following accretion.

The use of a single ^{26}Al/^{27}Al ratio for the initial heat generated implicitly assumes that Hebe accreted quickly ($\ll 10^6$ years) in the nebula in the manner described by Wetherill and Stewart (1993), who favored runaway growth timescales of only 10^5 years. Long accretion times, >1 Ma, would result in dramatically lower ^{26}Al/^{27}Al ratios for dust and debris that accreted late, as opposed to the initially accreted material. However, if the late accreting material had grown to small planetesimals before accreting then even this material could have retained much of the original heat produced from the decay of ^{26}Al. Accretion times that are much less than the 0.72 Ma half-life of ^{26}Al or longer accretion times for planetesimal-sized debris would be approximated adequately by an "instantaneous" accretion model.

MODEL PARAMETERS

Radiogenic Heat Sources

The heat source used in the model calculations was primarily the decay of ^{26}Al. Ghosh and McSween (1996) found that ^{60}Fe (half-life = 1.5 Ma) was not important compared to ^{26}Al in the internal heating of 4 Vesta, or probably the asteroid belt as a whole (Grimm and McSween 1993). Iron-60 becomes the dominant heat source after 5 Ma, at which time the heat generated by both ^{60}Fe and ^{26}Al is unimportant (Fig. 2). Aluminum-26 remains the most plausible means of heat generation in asteroids. Most CAI have ^{26}Al/^{27}Al ratios that cluster around 5×10^{-5}, but there are significant variations and some CAI contain no evidence for ^{26}Al. These variations may be due to heterogeneous distribution of ^{26}Al during CAI formation or to relatively long time spans in the early solar system. Podosek and Cassen (1994) and MacPherson *et al.* (1995) noted that ^{26}Al/^{27}Al ratios were probably reset by storage and reprocessing events in the nebula.

Aluminum-26 heat production was modeled by multiplying the initial ^{26}Al/^{27}Al ratio by 115 J g^{-1} yr^{-1}, the

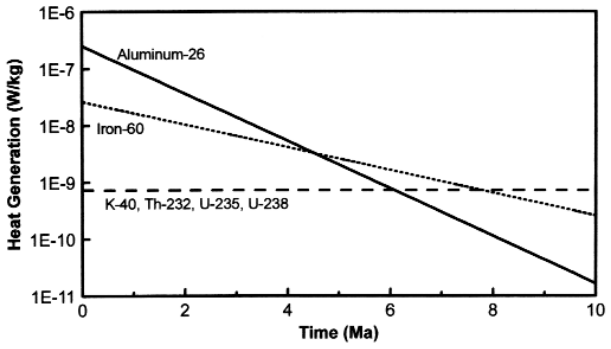

FIG. 2. Potential heat generation by short- and long-lived radionuclides with time after initial CAI formation. Initial ^{26}Al heat production is about 10 times greater than ^{60}Fe. Iron-60 becomes dominant only after 5 Ma, at which time the heat production of both aluminum-26 and iron-60 is insignificant. Heat generated by the long-lived isotopes only become significant after 8 Ma. Data from Herndon and Herndon (1977), Grimm and McSween (1993), and MacDonald (1959).

potential heat generated based on bulk Al content in H-chondrites (Herndon and Herndon 1977). The ^{26}Al/^{27}Al ratio was chosen (5.5×10^{-6}, corresponding to about 2.3 Ma after CAI formation) so that calculated internal temperatures matched the peak metamorphic temperatures for type 6 chondrites. The heat generated by the remaining radionuclides was determined by multiplying the decay energy by the rate of decay.

Internal Temperatures

The initial internal temperatures of the asteroids were assumed to be present day blackbody temperatures, which range from about 200 K near the inner portions of the belt to 160 K in the outer regions. Wood (1979) assumed a value of 170 K for a chondritic asteroid. Bennett and McSween (1996) used initial temperatures of 160 and 500 K, but assumed an initial value of 300 K for most of their work. We assume an initial internal temperature of 200 K, although the qualitative nature of the results is not sensitive to this value. Higher initial temperatures and lower ^{26}Al/^{27}Al ratios would also match the estimated peak temperatures.

A major constraint in the calculations is the peak metamorphic temperatures of the petrographic types. An upper limit is set by the absence of metal–troilite eutectics which form at ~1250 K (McSween *et al.* 1988). The least metamorphosed H-chondrites do not show characteristics of slow cooling through 673 K, suggesting metamorphic conditions below this temperature. Guimon *et al.* (1985) used the phase transformation from low to high feldspar in ordinary chondrites to establish the metamorphic temperature of type 3.5 at about 850 K. Dodd (1981) estimated metamorphic temperatures based on relative abundances of orthopyroxene and clinopyroxene grains and suggested temperatures for type 3 of ~870 K, type 4 of ~970 K, type 5 of ~1020 K, and type 6 of ~1220 K (McSween et al. 1988).

Thermal Conductivity, Density, and Porosity

The thermal evolution of Hebe is strongly dependent upon its modeled internal structure. Previous models have assumed uniform thermal conductivity throughout the body's interior (e.g., Herndon and Herndon 1977; Miyamoto *et al.* 1981). Regolith insulation reduces heat flow from a planetary interior (Warren and Rasmussen 1987), and Haack *et al.* (1990) reported that core cooling rates for differentiated asteroids were lowered by a factor of 10 and an asteroid's radius was reduced by a factor of 5 whenever the effects of regolith insulation were included. Lunar heat flow measurements have shown that the effective thermal conductivity of loosely consolidated regolith can be more than two orders of magnitude lower than for coherent rock (Langseth *et al.* 1976). The highly porous nature of the particulate materials prevents significant heat transport owing to the limited physical contact between grains (Presley and Christensen 1997).

Previous thermal models for chondritic asteroids have not included conditions for regolith insulation. Presumably this is due in large part to the difficulty in maintaining stable calculations across boundary regions (e.g., megaregolith–regolith). Wood (1979) noted similar difficulties in maintaining stable calculations when accreting dust onto a small chondritic body. The finite-difference method of integration can fail across large discontinuities in conductivity. The thermal conductivity values we used are based on the laboratory-measured physical characteristics for H-chondrites. Yomogida and Matsui (1983) measured the physical properties of chondrites including porosity, bulk density, and thermal diffusivity and obtained a relationship between these properties and thermal conductivity,

$$K = (A + B/T)\rho C_p(1–1.13\phi^{0.333}), \quad (6)$$

where K is the thermal conductivity, A and B are diffusivity coefficients for an H-chondrite, ρ is the bulk density, C_p is the heat capacity, and ϕ is the porosity (Yomogida and Matsui 1984). This expression overestimates the conductivity of the lunar regolith (Warren and Rasmussen 1987), but is applicable to chondrites. Attempts at lowering the conductivity values resulted in unstable calculations due to large jumps in conductivity and porosity at boundaries (Wood 1979).

For most calculations, the diffusivity coefficients of H6 Gladstone were used (Yomogida and Matsui 1983). The density and porosity were defined by radial position within the body. In the interior (Fig. 1), bulk density was taken as 3000–3500 kg m^{-3} (Yomogida and Matsui 1983) and a

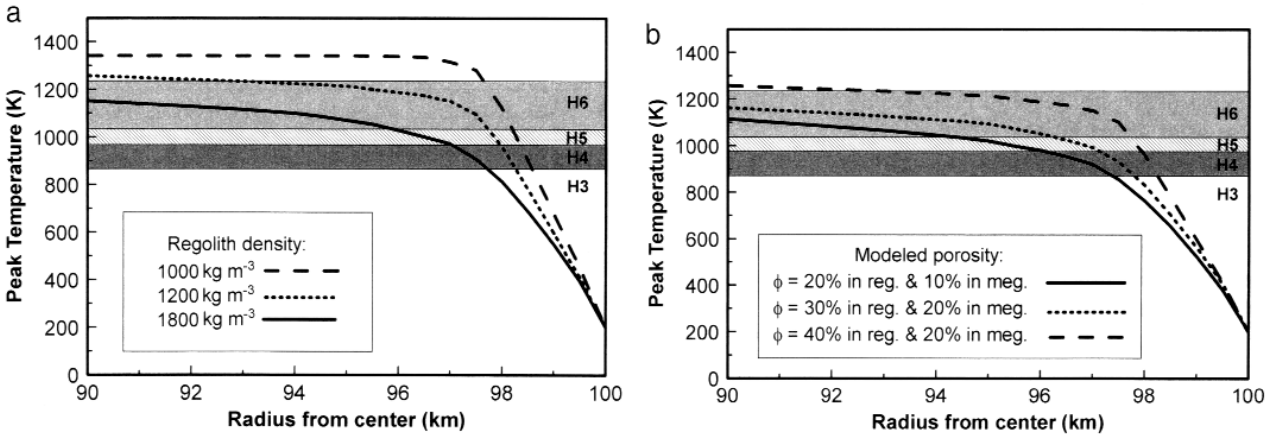

FIG. 3. Peak temperature profiles for Hebe assuming a 2.5 km thick regolith. (a) Curves represent three regolith density models. High regolith density results in faster heat transfer and lower peak temperature. Also plotted are the relevant zones for the lesser metamorphosed types. (b) Curves represent three regolith and megaregolith porosity models. High regolith and megaregolith porosity serve to insulate the interior, resulting in a steep temperature gradient near the surface. The shallow burial depths indicate that H-chondrites may originate in a regolith/megaregolith environment before ejection from the parent body by impact.

porosity of 6% is used, an average value for H6 chondrites (Yomogida and Matsui 1983; Britt *et al.* 1995). The bulk density of the megaregolith, modeled as a transition zone between the consolidated interior and the unconsolidated regolith, was taken as 2200–2800 kg m^{-3} and porosity increased to 20–30%. Regolith was assumed to have density 1200–1800 kg m^{-3} and 40–60% porosity (Carrier *et al.* 1991). The dependence of the heat capacity upon temperature was approximated using an empirical equation for forsterite in the 298–1800 K temperature range (Robie *et al.* 1979).

RESULTS

Regolith Insulation Effects

The incorporation of regolith characteristics in the numerical calculations for the surface layer dramatically alters the predicted thermal evolution of Hebe. The insulating properties of the regolith slow the heat flow from the interior. The slowed cooling of the interior results in a large volume of material which experienced the maximum temperature of ~1250 K. Figure 3 shows that >95% of Hebe's volume may have experienced temperatures corresponding to H-chondrites of petrographic type 6. The surface radiation boundary condition results in a steep temperature gradient between the insulated hot interior and cool surface. Figure 3 indicates that burial depths for H-chondrites can be surprisingly shallow, although some H6 may have had deep burial. Essentially all H-chondrites could be derived from the upper few km of the parent body and may represent lithified regolith material.

The significant differences between heating models for regolith-covered bodies and solid bodies are shown in Fig. 4. In our model, 10 km depth is just below the base of the megaregolith. The regolith provides sufficient insulation during the decay of ^{26}Al so that the peak temperature experienced by material just below the regolith/megaregolith zones is nearly identical to that at the center of Hebe. With no regolith, the greater thermal conductivity of coherent rock results in substantial cooling coinciding with the initial heating stage. The 400 K difference in peak temperatures between regolith-covered bodies and nonlayered

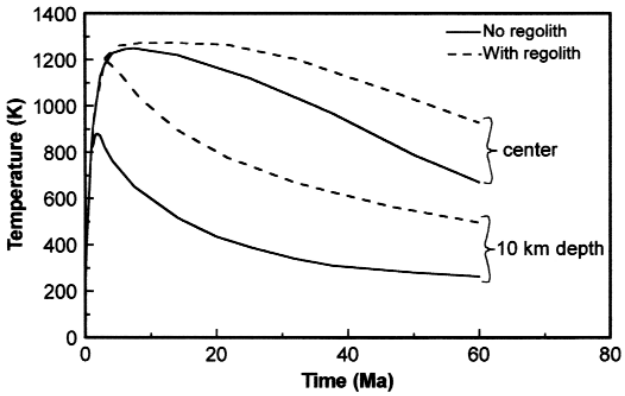

FIG. 4. Two model runs showing effects of regolith insulation at 10 km below the surface and at the center of the body. Solid lines represent Hebe with no surface regolith. Dashed lines represent Hebe with a 2.5 km regolith. Cooling rates are slower with regolith insulation and result in significant differences in modeled temperature after 60 Ma.

bodies results in a considerably different thermal structure for Hebe. Near the center of the body the peak temperatures of the two models are nearly the same, but faster cooling of the nonregolith body results in a 200 K difference after about 60 Ma.

Cooling Rates

Estimates of the cooling rates for H-chondrites have been used to constrain parent body size (e.g., Wood 1967) and to argue both for and against an inverse correlation with petrographic type (e.g., Lipschutz *et al.* 1989; Taylor *et al.* 1987). The primary assumption in comparing cooling rates with petrographic type is that the onion-shell structure was established prior to mixing or breakup from impacts. Heating by radioactive decay would create a range of peak metamorphic temperatures corresponding to the observed petrographic types in chondrites. This shell model implies increased metamorphism and lowered cooling rates with depth in the parent body. Meteorites undisturbed during the cooling phase should show effects of slow cooling that correlates with burial depth.

Table I compares the measured cooling rates for H-chondrites obtained by metallographic diffusion of nickel in metal through the 870–670 K range. Cooling rates tend to decrease with petrographic type, as would be expected from an onion-shell model for metamorphism. Although the slowest cooling rates for each class are similar (~10 K/Ma), there is an order of magnitude difference in the maximum cooling rates for each class (H4 > 1000 K/Ma, H5 ~ 200 K/Ma, and H6 ~ 10 K/Ma). Antarctic H4 and H5 tend to show higher cooling rates than the non-Antarctic H-chondrites. Meteorites collected from the Antarctic have long terrestrial histories due to an environment conducive to storage. Benoit and Sears (1993; 1996) found a significant number of Antarctic H-chondrites with thermal histories substantially different than those for modern H-chondrite falls. Thermal models using cooling rates derived from modern falls alone may be biased against H4 and H5 with faster cooling rates. Some unshocked H4 have very fast metallographic cooling rates in excess of 1000 K/Ma, which suggests primary cooling. For example, Forest Vale has a cooling rate >1000 K/Ma and an ancient Ar–Ar age of 4.52 Ga (Turner *et al.* 1978) indicating that it has not been reheated above 500 K since its initial closure. Cooling rates of this magnitude are difficult to obtain with any numerical model and may be the result of impact excavation of hot material from depth and exposure on or near the surface of the parent body. Cooling rates between 1 and 150 K/Ma seem to be more indicative of the slow cooling expected from radiogenic heating.

Figure 5 illustrates the cooling rate as a function of depth within Hebe modeled with various regolith thicknesses. The cooling curves are based on cooling between 870 and 670 K so that comparisons can be made directly with metallographic and fission track data. For shallow burial of H-chondrites as predicted in Fig. 3, the modeled cooling rates agree well with observed values in H-chondrites. The dashed line represents the extrapolated cooling curve since maximum temperatures near the surface for a body with no regolith did not reach 870 K. The addition of a regolith results in a factor of 10 decrease in cooling rate for depths ≥10 km; greater differences are found at <10 km. Cooling rates near the surface vary significantly and depend on the thickness of the surrounding regolith.

TABLE I
Metallographic Cooling Rates for Unshocked H-Chondrites Determined in the 870–670 K Range

Meteorite	Class	Cooling rate (K/Ma)[a]
Ankober	H4	(5)[b]
ALHA81105	H4	10[c]
Sena	H4	20
Conquista	H4	25[c]
ALHA78134	H4	50[c]
ALHA80121	H4	50[c]
ALHA77262	H4	100
ALHA79035	H4	100
ALHA81092	H4	130[c]
ALHA80131	H4	150[c]
Ste. Marguerite	H4	>1000
Forest Vale	H4	>1000
ALHA78115	H5	10
Allegan	H5	15
Nuevo Mercurio	H5	15
Richardton	H5	20
ALHA77294	H5	20–30
ALHA78111	H5	30–50
Nadiabondi	H5	50[c]
ALHA79026	H5	200
Guarena	H6	4.6
ALHA76008	H6	5
ALHA78076	H6	10
Kernouve	H6	10
Estacado	H6	10

[a] Data from Lipschutz *et al.* (1989), Benoit and Sears (1993; 1996).
[b] Brackets indicate some scatter in the result.
[c] Unknown shock, classification; all other meteorites listed have shock values S1–2 or a–b (Koblitz 1997).

Pb–Pb Closure Times

The formation ages of chondrites can also help constrain cooling rate information and provide clues to the structure of the H-chondrite parent body. Formation ages or closure times for minerals are usually determined by radiogenic decay where the daughter product is retained within the system below some critical temperature. For parent body metamorphism, the formation age would reflect the time

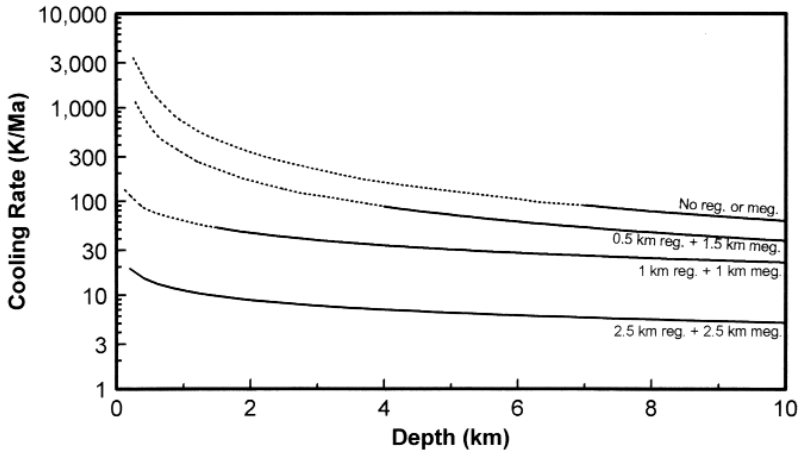

FIG. 5. Cooling rate curves for Hebe modeled with various regolith and megaregolith thicknesses. At any given depth within Hebe there is about a factor of 10 difference between a thick modeled regolith and no regolith. The cooling rate curves are calculated for the temperature region 870–670 K for comparison to metallographic cooling rates obtained from H-chondrites. Dashed lines represent extrapolated cooling curves since the maximum temperature at these shallow depths did not reach 870 K in the numerical model. Curves would also be appropriate for cooling after impact heating.

at which the solids cooled below the closure temperature. Meteorites that formed near the surface of their parent body should exhibit faster cooling rates and older formation times. Deeply buried material would retain heat longer and may require millions of years to reach the closure temperature. The onion-shell model predicts younger ages with greater depth within the parent body.

Göpel *et al.* (1994) measured the Pb–Pb ages of phosphates in equilibrated ordinary chondrites (Table II). The closure times for the H-chondrites seem to correlate with degree of metamorphism. The H4 chondrite Ste. Marguerite reached the closure temperature (690–750 K) about 60 Ma before H6 Guarena, indicating that the more deeply buried H6 required longer times to cool through the closure temperature, consistent with our numerical model. Table II shows the formation times of H-chondrites relative to the H4 closure of U–Pb. The closure times are based on a numerical model assuming of a 3 km thick regolith. Formation times for H6 reflect burial depths between 3 and 8 km. The model ages agree well with those observed in H-chondrites if the material originated at shallow depths with some overlying regolith as would be expected. If no regolith were ever present (an unlikely case) the observed cooling rates would require burial at greater depths, on the order of 60 km.

TABLE II
Pb–Pb Closure Ages for H-Chondrites and Predictions by Present Model

	Pb–Pb Age[a] (Ga)	Model depth (km)	Δt[b] (Ma)
H5 chondrites			
Allegan	4.5563		6.7
Richardton	4.5534		9.6
Current study (3 km regolith)		2.3	10.5
Current study (no regolith)		18	4.1
H6 chondrites			
Kernouve	4.5214		41.6
Guarena	4.5056		57.4
Current study (3 km regolith)		3–8	40–52
Current study (no regolith)		57–100	40–53

[a] Pb–Pb ages from Göpel *et al.* (1994).
[b] Chondrite Δt w.r.t. H4 Ste. Marguerite (Pb–Pb age = 4.5630 Ga).

DISCUSSION

Burial Depths

The original position of H-chondrites inside the parent body is a simple but fundamental question. Estimates of burial depth for each petrologic type vary widely and depend upon the choice of input parameters for the thermal model used. We have estimated burial depths in our model by using the observed peak metamorphic temperature for each class as the upper boundary between that class and the next higher metamorphosed class. Models using ^{26}Al heating result in an onion-shell layering where there is an inverse correlation between degree of metamorphism and the cooling rate. Some have suggested that evidence supporting this trend in H-chondrites can be found in metallographic, fission track, and induced thermoluminescence

data (Lipschutz *et al.* 1989; Benoit *et al.* 1997). Others (e.g., Taylor *et al.* 1987; Keil *et al.* 1994) have argued that no trend exists between metallographic cooling rates and metamorphic type.

Models that employ single values for thermal diffusivity and other thermal parameters seem to indicate deep burial for H6 chondrites. Miyamoto *et al.* (1981) found in their calculations that H6 required burial depths greater than 30 km on an 85 km radius parent body. Bennett and McSween (1996) revised Miyamoto *et al.*'s calculations using variable diffusivity and ultimately moved each of the petrographic type boundaries closer to the surface (Table III). They found burial depths for H6 to be >6 km on an uncompacted (high porosity) body of radius 56 km and >10 km for a compacted (low porosity) body of radius 93 km. Taylor *et al.* (1987) used the cooling model of Wood (1967) to argue for burial of ordinary chondrites that cooled at 10 K/Ma to be >40 km on a body of >50 km radius.

Our results suggest that H-chondrites could form at very shallow depths even for the most highly metamorphosed type 6 H-chondrites. The insulating properties of a surface regolith move each of the petrographic zones nearer to the surface (Fig. 6). The model indicates that most of the body is composed of H6 material, extending to the outermost few km of the body. We estimate that the H4 and H5 chondrites compose only 5.6 vol% of the proposed parent body, while H4 and H5 chondrites make up about 65% of the H-chondrite falls (Koblitz 1997). However, meteorite fall biases caused by atmospheric passage and ejection mechanisms from the parent body result in a non-representative sampling of the asteroid belt (Sears 1998). Benoit and Sears (1993) have shown using induced thermoluminescence data from Antarctic meteorites that the H-chondrite flux has changed over the last 10^6 years. Current fall statistics of H-chondrites are almost certainly not representative of parent body stratigraphy.

In support of the shallow burial of most H-chondrites is the abundance of regolith breccias and meteorites containing implanted solar wind gases. Many breccias contain mixtures of type 3–6 components (Lipschutz *et al.* 1983; Bunch and Rajan 1988) suggesting extensive mixing of material presumably originating in different locations on the parent body. Lipschutz *et al.* (1993) found that the Noblesville breccia contained H6 clasts embedded in an H4 matrix with an especially high amount of solar gases. The common occurrence of H-chondrites containing solar gases (14% by number) requires extensive residence times on the surface of the parent body (Crabb and Schultz 1981). Figure 7 shows a distribution of H-chondrites containing solar gases and their cosmic-ray exposure age. There is a strong peak at ~8 Ma and the overall distribution of ages is similar to the H-chondrite population as a whole (Graf and Marti 1995). The peak at 8 Ma is interpreted to indicate a single impact event that produced numerous ~1 m meteoroids. This impact event sampled petrologic types 3–6 with 43% of these containing solar gases, suggesting impact and ejection of regolith material.

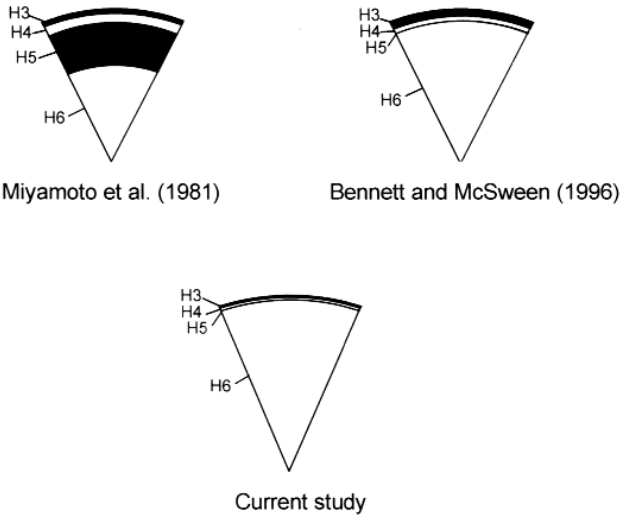

FIG. 6. Comparison of numerically modeled petrographic type regions. The present model, with a 2.5 km thick regolith, indicates that types 3–6 can be formed near the surface in a regolith and megaregolith environment. Previous models required deeper burial for type 6 material.

TABLE III
Comparisons between Three Thermal Models for the H-Chondrite Parent Body

	Radii (km)[a]	Vol. %[a]	Radii (km)[b]	Vol. %[b]	Radii (km)[c]	Vol. %[c]
Total	85	100	88	100	100	100
H3	82.5	8.6	82.45	17.75	98.0	5.88
H4	77	17.1	80.5	5.70	97.2	2.30
H5	55	47.2	79.1	3.92	96.0	3.35
H6	0	27.1	0	72.62	0	88.47

[a] Miyamoto *et al.* (1981).
[b] Bennett and McSween (1996), compacted model.
[c] Current study.

Cooling Rate and Parent Body Structure

The rapid cooling rates (>1000 K/Ma) derived for the H4 chondrites Forest Vale and Ste. Marguerite would be difficult to obtain from simple cooling after ^{26}Al heating. For these fast cooling rates it seems likely that impact heating and mixing are responsible. Impacts prior to cooling would disrupt the shell model by excavating material from great depth resulting in fast cooling for highly metamorphosed material. Impact heating could imprint new

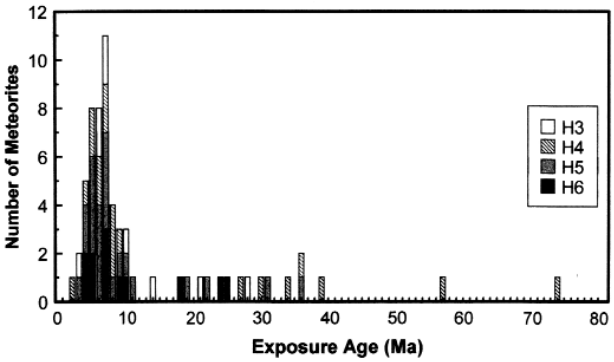

FIG. 7. Cosmic ray exposure ages of H-chrondrites containing solar gases. The distribution is similar to the overall H-chondrite population. The strong peak at ~8 Ma represents a single impact ejecting material of petrographic types 3–6 of which a significant amount contained solar wind. Exposure to the solar wind requires extensive surface residence times of even the highly metamorphosed material. (Data from Graf and Marti 1995.)

cooling rates on both individual clasts and whole rocks. The cooling rate of excavated material depends on its peak temperature following impact and its burial depth following deposition. Material deposited near the surface would cool quickly regardless of its initial burial position in the onion-shell structure. The extrapolated cooling rate curve (dashed line) for a body with no regolith in Fig. 5 should approximate the cooling experienced by material deposited near the surface. The extrapolation is included since curves are also valid for cooling after impact.

It is also possible that some of the metamorphism and cooling rates may be the result of impact heating of the surface. The cooling curves shown in Fig. 5 are not sensitive to the nature of the heat source. Both ^{26}Al and impacts deposit large amounts of heat into a regolith, creating concentric zones of metamorphism around the heat source. Cooling rates from both heat sources would be primarily dependent on burial depth of the material. Deep burial inside a thick regolith could lower cooling rates by a factor of 100 over shallow burial in thin regoliths. Smith and Goldstein (1977) found two shocked blackened H-chondrites with extremely fast metallographic cooling rates that were interpreted to represent rapid cooling at shallow burial depths. The cooling rates of H5 Rose City and H6 Orvinio were 1 K/yr and 100 K/day, respectively, corresponding to burial depths of <100 m. Sears *et al.* (1997) used induced thermoluminescence data to conclude that the HED meteorites experienced shock heating and cooled in a regolith varying between 0 and ~2 km in depth.

The occurrence of highly metamorphosed regolith breccias is seemingly contradictory to previous onion-shell models of parent body stratigraphy. Type 6 material is thought to have originated at depths well below the surface regolith. To remedy this apparent inconsistency numerous individuals have invoked fragmentation and reassembly of the entire parent body (e.g., Scott and Rajan 1981; Grimm 1985; Taylor *et al.* 1987; Keil *et al.* 1994). Impact disruption would create "rubble piles" of mixed type 3–6 material upon reaccretion. This hypothesis allows for the excavation of deeply buried material and can result in a variety of cooling rates for individual grains shocked to high temperature (Taylor *et al.* 1987). Our model also predicts that H5–6 material could be derived from great depth (Table II) if little or no regolith cover exists on the parent body.

We suggest a possible alternative to the catastrophic fragmentation and reaccretion scenario. The addition of regolith insulation in the numerical models results in potentially shallow burial depths for all H-chondrites. In fact, the model can accommodate all the petrographic types in the regolith/upper megaregolith regions. Small noncatastrophic impacts into Hebe's surface could easily excavate and expose type 6 material to the surface. For impacts occurring after the primary metamorphism, cooling rates of individual grains would reflect their post-depositional environment. Deep burial results in slower cooling than for material exposed on or near the surface. Impact gardening and turnover of the regolith could account for the abundance of regolith breccias and solar gas bearing H-chondrites. Huang *et al.* (1996) have proposed the origins of ordinary chondrites to be in dusty regolith environments to allow for the observed metal–silicate fractionation. There would seem to be no requirement that the H-chondrite parent body (Hebe) have an internal rubble pile structure.

ACKNOWLEDGMENTS

We thank two anonymous reviewers for constructive reviews. John Wood also provided valuable comments on the thermal model.

REFERENCES

Akridge G., P. H. Benoit, and D. W. G. Sears 1997. The thermal history of 6 Hebe as the H-chondrite parent body [abstract]. *Lunar Planet. Sci.* **28,** 13–14.

Allan, D. W. 1955. Heat in the earth. *Advances. Sci.* **12,** 89–96.

Asphaug, E., and M. C. Nolan 1992. Analytical and numerical predictions for regolith production on asteroids [abstract]. *Lunar Planet. Sci.* **23,** 43–44.

Belton, M. J. S., and 19 colleagues 1994. First images of asteroid 243 Ida. *Science* **265,** 1543–1547.

Bennett, M. E., and H. Y. McSween, Jr. 1996. Revised model calculations for the thermal histories of ordinary chondrite parent bodies. *Meteorit. Planet. Sci.* **31,** 783–792.

Benoit, P. H., and D. W. G. Sears 1993. Breakup and structure of an H-chondrite parent body: The H-chondrite flux over the last million years. *Icarus* **101,** 188–200.

Benoit, P. H., and D. W. G. Sears 1996. Rapid changes in the nature of the H chondrites falling to Earth. *Meteorit. Planet. Sci.* **31,** 81–86.

Benoit, P. H., Y. Chen, and D. W. G. Sears 1997. The cooling history and structure of the ordinary chondrite parent bodies. *Meteoritics Planet. Sci.*, submitted.

Britt, D. T., D. A. Kring, and J. F. Bell 1995. The density/porosity of asteroids [abstract]. *Lunar Planet. Sci.* **26,** 177–178.

Bunch, T. E., and R. S. Rajan 1988. Meteorite regolithic breccias. In *Meteorites and the Early Solar System* (J. F. Kerridge and M. S. Matthews, Eds.), pp. 144–164. Univ. of Arizona Press, Tucson.

Carr, M. H., R. L. Kirk, A. McEwen, J. Ververka, P. Thomas, J. W. Head, and S. Murchie 1994. The geology of Gaspra. *Icarus* **107,** 61–71.

Carrier, W. D., Jr., G. R. Olhoeft, and W. Mendell 1991. Physical properties of the lunar surface. In *Lunar Sourcebook: A User's Guide to the Moon* (G. Heiken, D. Vaniman, and B. M. French, Eds.), pp. 475–594. Cambridge Univ. Press, Cambridge.

Crabb, J., and L. Schultz 1981. Cosmic-ray exposure ages of the ordinary chondrites and their significance for parent body stratigraphy. *Geochim. Cosmochim. Acta* **45,** 2151–2160.

Dodd, R. T. 1981. *Meteorites: A Petrologic–Chemical Synthesis.* Cambridge Univ. Press, Cambridge.

Farinella, P., C. Froeschlè, and R. Gonczi 1993. Meteorites from the asteroid 6 Hebe. *Celest. Mech. Dynam. Astron.* **56,** 287–305.

Gaffey, M. J. 1996. Spectral identification of asteroid 6 Hebe as the main-belt parent body of the H-type ordinary chondrites [abstract]. *Meteoritics* **31,** A47.

Gaffey, M. J., and S. L. Gilbert 1997. Asteroid 6 Hebe: The probable parent body of the H-type ordinary chondrites and the IIE iron meteorites. *Meteoritics Planet. Sci.*, submitted.

Ghosh, A., and H. Y. McSween, Jr. 1996. The thermal history of asteroid 4 Vesta, based on radionuclide and collisional heating [abstract]. In *Workshop on Evolution of Igneous Asteroids: Focus on Vesta and the HED Meteorites*, pp. 9–10, LPI Technical Report 96–02. Lunar Planetary Institute, Houston.

Göpel, C., G. Manhès, and C. J. Allègre 1994. U–Pb systematics of phosphates from equilibrated ordinary chondrites. *Earth Planet. Sci. Lett.* **121,** 153–171.

Graf, T., and K. Marti 1995. Collisional history of H chondrites. *J. Geophys. Res.* **100,** 21,247–21,263.

Grimm, R. E. 1985. Penecontemporaneous metamorphism, fragmentation, and reassembly of ordinary chondrite parent bodies. *J. Geophys. Res.* **90,** 2022–2028.

Grimm, R. E., and H. Y. McSween, Jr. 1993. Heliocentric zoning of the asteroid belt by aluminum-26 heating. *Science* **259,** 653–655.

Guimon, R. K., B. D. Keck, K. S. Weeks, J. DeHart, and D. W. G. Sears 1985. Chemical and physical studies of type 3 chondrites. IV. Annealing studies of a type 3.4 ordinary chondrite and the metamorphic history of meteorites. *Geochim. Cosmochim. Acta* **49,** 1515–1524.

Haack, H., K. L. Rasmussen, and P. H. Warren 1990. Effects of regolith/megaregolith insulation on the cooling histories of differentiated asteroids. *J. Geophys. Res.* **95,** 5111–5124.

Herbert, F., C. P. Sonett, and M. J. Gaffey 1991. Protoplanetary thermal metamorphism: The hypothesis of electromagnetic induction in the protosolar wind. In *The Sun in Time* (C. P. Sonett, M. S. Giampapa, and M. S. Matthews, Eds.), pp. 710–739. University of Arizona Press, Tucson.

Herndon, J. M., and M. A. Herndon 1977. Aluminum-26 as a planetoid heat source in the early Solar System. *Meteoritics* **12,** 459–465.

Housen, K. R. 1992. Crater ejecta velocities for impacts on rocky bodies [abstract]. *Lunar Planet. Sci.* **23,** 555–556.

Housen, K. R., L. L. Wilkening, C. R. Chapman, and R. J. Greenberg 1979. Asteroidal regoliths. *Icarus* **39,** 317–351.

Huang, S., G. Akridge, D. W. G. Sears 1996. Metal–silicate fractionation in the surface dust layers of accreting planetesimals: Implications for the formation of ordinary chondrites and the nature of asteroid surfaces. *J. Geophys. Res.* **101,** 29,373–29,385.

Keil, K., H. Haack, and E. R. D. Scott 1994. Catastrophic fragmentation of asteroids: Evidence from meteorites. *Planet. Space Sci.* **42,** 1109–1122.

Keil, K., D. Stoffler, S. G. Love, and E. R. D. Scott 1997. Constraints on the role of impact heating and melting in asteroids. *Meteoritics Planet. Sci.* **32,** 349–363.

Koblitz, J. 1997. *MetBase, Meteorite Data Retrieval Program, version 3.0.* J. Koblitz, Fisherlude, Germany.

Langevin, Y., and M. Maurette 1980. A model for small body regolith evolution: The critical parameters [abstract]. *Lunar Planet. Sci.* **9,** 602–604.

Langseth, M. G., S. J. Keihm, and K. Peters 1976. Revised lunar heat-flow values. *Proc. Lunar Sci. Conf.* **7,** 3143–3171.

Lee, T., D. A. Papanastassiou, and G. J. Wasserburg 1976. Demonstration of ^{26}Mg excess in Allende and evidence for ^{26}Al. *Geophys. Res. Lett.* **3,** 41–44.

Lipschutz, M. E., S. Biswas, and H. McSween 1983. Chemical characteristics and origin of H chondrite regolith breccias. *Geochim. Cosmochim. Acta* **47,** 169–179.

Lipschutz, M. E., M. J. Gaffey, and P. Pellas 1989. Meteorite parent bodies: Nature, number, size and relation to present-day asteroids. In *Asteroids II* (R. P. Binzel, T. Gehrels, and M. S. Matthews, Eds.), pp. 740–777. Univ. of Arizona Press, Tucson.

Lipschutz, M. E., and 16 colleagues 1993. Consortium study of the unusual H chondrite regolith breccia, Noblesville. *Meteoritics* **28,** 528–537.

MacDonald, G. J. F. 1959. Calculations on the thermal history of the Earth. *J. Geophys. Res.* **64,** 1967–2000.

MacPherson, G. J., A. M. Davis, and E. K. Zinner 1995. The distribution of aluminum-26 in the early Solar System—A reappraisal. *Meteoritics* **30,** 365–386.

McKay, D. S., G. Heiken, A. Basu, G. Blanford, S. Simon, R. Reedy, B. M. French, and J. Papike 1991. The lunar regolith. In *Lunar Sourcebook: A User's Guide to the Moon* (G. H. Heiken, D. T. Vaniman, and B. M. French, Eds.), pp. 285–356. Cambridge Univ. Press, Cambridge.

McSween, H. Y., D. W. G. Sears, and R. T. Dodd 1988. Thermal metamorphism. In *Meteorites and the Early Solar System* (J. R. Kerridge and M. S. Matthews, Eds.), pp. 102–113. Univ. of Arizona Press, Tucson.

Migliorini, F., A. Manara, F. Scaltritti, P. Farinella, A. Cellino, and M. Di Martino 1997. Surface properties of (6) Hebe: A possible parent body of ordinary chondrites. *Icarus* **128,** 104–113.

Minster, J., and C. J. Allègre 1979. ^{87}Rb–^{87}Sr chronology of H chondrites: Constraint and speculations on the early evolution of their parent body. *Earth Planet. Sci. Lett.* **42,** 333–347.

Morbidelli, A., R. Gonczi, C. Froeschle, and P. Farinella 1994. Delivery of meteorites through the ν_6 secular resonance. *Astron. Astrophys.* **282,** 955–979.

Miyamoto, M., N. Fujii, and H. Takeda 1981. Ordinary chondrite parent body: An internal heating model. *Proc. Lunar Planet Sci.* **12,** 1145–1152.

Podosek, F. A., and P. Cassen 1994. Theoretical, observational, and isotopic estimates of the lifetime of the solar nebula. *Meteoritics* **29,** 6–25.

Presley, M. A., and P. R. Christensen 1997. Thermal conductivity measurements of particulate materials. 1. A review. *J. Geophys. Res.* **102,** 6535–6549.

Reynolds, R. T., P. E. Fricker, and A. L. Summers 1966. Effects of melting upon the thermal models of the earth. *J. Geophys. Res.* **71,** 573–582.

Robie, R. A., B. S. Hemingway, and J. R. Fisher 1979. *Thermodynamic Properties of Minerals and Related Substances at 298.15 K and 1 bar*

(10^5 Pascals) Pressure and at Higher Temperatures. Geological Survey Bulletin 1452, Washington, D. C.

Rubin, A. E. 1995. Petrologic evidence for collisional heating of chondritic asteroids. *Icarus* **113,** 156–167.

Russell, S. S., G. Srinivasan, G. R. Huss, G. J. Wasserburg, and G. J. MacPherson 1996. Evidence for widespread ^{26}Al in the solar nebula and constraints for nebula time scales. *Science* **273,** 757–762.

Scott, E. R. D., and R. S. Rajan 1981. Metallic minerals, thermal histories, and parent bodies of some xenolithic, ordinary chondrites. *Geochim. Cosmochim. Acta* **45,** 53–67.

Sears, D. W. G. 1998. The case for chondrules and CAI being rare in the early solar system and some implications for astrophysical models. *Astrophys. J.,* in press.

Sears, D. W. G., and R. T. Dodd 1988. Overview and classification of meteorites. In *Meteorites and the Early Solar System* (J. F. Kerridge and M. S. Matthews, Eds.), pp. 3–31. Univ. of Arizona Press, Tucson.

Sears, D. W. G., S. J. K. Symes, J. D. Batchelor, D. G. Akridge, and P. H. Benoit 1997. The metamorphic history of eucrites and eucrite-related meteorites and the case for late metamorphism. *Meteorit. Planet. Sci.* **32,** 917–927.

Shukolyukov, A., and G. W. Lugmair 1992. First evidence for live ^{60}Fe in the solar system [abstract]. *Lunar Planet. Sci.* **23,** 1295–1296.

Smith, B. A., and J. I. Goldstein 1977. The metallic microstructures and thermal histories of severely reheated chondrites. *Geochim. Cosmochim. Acta* **41,** 1061–1072.

Taylor, G. J., P. Maggiore, E. R. D. Scott, A. E. Rubin, and K. Keil 1987. Original structures, and fragmentation and reassembly histories of asteroids: Evidence from meteorites. *Icarus* **69,** 1–13.

Turner, G., M. C. Enright, and P. H. Cadogan 1978. The early history of chondrite parent bodies inferred from ^{40}Ar–^{39}Ar ages. *Proc. Lunar Planet. Sci.* **9,** 989–1025.

Warren, P. H., and K. L. Rasmussen 1987. Megaregolith insulation, internal temperatures, and bulk uranium content of the moon. *J. Geophys. Res.* **92,** 3453–3465.

Wetherill, G. W., and G. R. Stewart 1993. Formation of planetary embryos: Effects of fragmentation, low relative velocity, and independent variation of eccentricity and inclination. *Icarus* **106,** 190–209.

Wood, J. A. 1967. Chondrites: Their metallic minerals, thermal histories, and parent planets. *Icarus* **6,** 1–49.

Wood, J. A. 1979. Review of metallographic cooling rates of meteorites and a new model for the planetesimals in which they formed. In *Asteroids* (T. Gehrels, Ed.), pp. 849–891. Univ. of Arizona Press, Tucson.

Wood, J. A., and P. Pellas 1991. What heated the parent meteorite planets? In *The Sun in Time* (C. P. Sonett, M. S. Giampapa, and M. S. Matthews, Eds.), pp. 740–760. Univ. of Arizona Press, Tucson.

Yomogida, K., and T. Matsui 1983. Physical properties of ordinary chondrites. *J. Geophys. Res.* **88,** 9513–9533.

Yomogida, K., and T. Matsui 1984. Multiple parent bodies of ordinary chondrites. *Earth Planet. Sci. Lett.* **68,** 34–42.